Level structure of ^{220}Ra

J. F. Shriner, Jr., P. D. Cottle, J. F. Ennis, M. Gai, and D. A. Bromley
A.W. Wright Nuclear Structure Laboratory, Yale University, New Haven, Connecticut 06511

J. W. Olness and E. K. Warburton
Department of Physics, Brookhaven National Laboratory, Upton, New York 11973

L. Hildingsson, M. A. Quader, and D. B. Fossan
Department of Physics, State University of New York, Stony Brook, New York 11794
(Received 16 August 1985)

A level scheme for ^{220}Ra is presented, established using the ^{208}Pb(^{14}C,2n) reaction studied near the Coulomb barrier ($60 \leq E \leq 68$ MeV). Measurements included γ-ray excitation functions, γ-γ coincidences, and γ-ray angular distributions. The dominant features in the spectrum are states of alternating parity connected by fast $E1$ transitions. Values of $B(E1)/B(E2)$ are obtained for states with $J = 6$–$17\hbar$. Examination of the systematic behavior of even-even Ra isotopes reveals a sharp change in structure as one proceeds from ^{214}Ra to ^{226}Ra. Results are discussed in terms of alpha-particle clustering (in particular as described by the vibron model) and of a stable octupole deformation; calculations of the energy spectrum based on the vibron model are presented.

I. INTRODUCTION

The existence of low-lying 1^- states in Ra and Th isotopes has long been known from alpha-particle decay studies.[1] However, only recently has the combination of heavy-ion-induced reactions and gamma-ray spectroscopic techniques been applied to extend our knowledge of nuclei in this region. These studies have stimulated renewed interest in the structure of these nuclei and have raised new questions about our understanding of the negative parity states.

As level schemes have been extended to states of higher spin, new features have emerged. Both ^{218}Ra (Refs. 2–5) and ^{222}Th (Refs. 6 and 7) show states of alternating parity at high spins. In addition, the $E1$ matrix elements linking these states are strongly enhanced. Recent theoretical interpretations of these phenomena have primarily followed two paths. One is the alpha-clustering model of Iachello and Jackson;[8] here the presence of the cluster separates the center-of-charge from the center-of-mass, leading to enhanced $E1$ matrix elements. This model also predicts low-lying negative-parity states and small alpha-particle decay hindrance factors, both of which are experimentally observed in this region. Calculations performed within this framework[9,10] show generally good agreement with both measured energy levels and $B(E1)/B(E2)$ ratios for Ra and Th isotopes.

The other current theoretical approach to explaining the structure of these nuclei interprets them in terms of a stable octupole deformation.[11–14] In this model the enhancement of $E1$ transitions arises from the fact that the octupole shape causes polarization of the nucleus[15,16] and thus displaces the center of charge from the center of mass, again giving a dipole moment. In addition, $E2$ and $E3$ matrix elements are enhanced. Since the alpha-cluster model also predicts enhancement of $E2$ and $E3$ matrix elements,[17] the two models appear to be related. However, it is not yet clear exactly what the relationship is or where salient differences occur, if anywhere.

In this paper we present data for ^{220}Ra and thus extend the knowledge of high spin states in even-even Ra isotopes another step away from the $N=126$ shell closure. We will examine the systematic behavior of these isotopes in terms of both excitation energies and $B(E1)/B(E2)$ ratios, where such data are available. Finally, calculations, based on the vibron model,[8] of energy levels for $^{220-226}$Ra will be presented, and we will show that the yrast levels of these four nuclei can be well reproduced by varying only one parameter in our fit. Two other studies[18,19] of ^{220}Ra have been reported with partial overlap to the present work; a preliminary version of the present work has been published.[20]

II. EXPERIMENTAL PROCEDURE

We studied ^{220}Ra via the ^{208}Pb(^{14}C,2n)^{220}Ra reaction, using the ^{14}C beam from the Brookhaven National Laboratory MP-7 tandem Van de Graaff accelerator. Experimental measurements included γ-ray excitation functions, γ-γ coincidences, and γ-ray angular distributions. Both thick (50 mg/cm^2) and thin (300 μg/cm^2 on 225 μg/cm^2 Au) targets of enriched ^{208}Pb were employed for the excitation function measurements. Beam energies ranged from 60 to 78 MeV; over this energy range the primary evaporation residues are ^{220}Ra, ^{219}Ra, and ^{218}Ra, corresponding to the 2n, 3n, and 4n channels, respectively. The excitation functions are shown in Fig. 1.

The thin target excitation functions showed clear evidence for the production of ^{219}Ra and ^{218}Ra. However, the γ rays expected from ^{220}Ra according to a previous alpha-decay study[21] were partially obscured by γ rays from reactions with the gold target backing and from

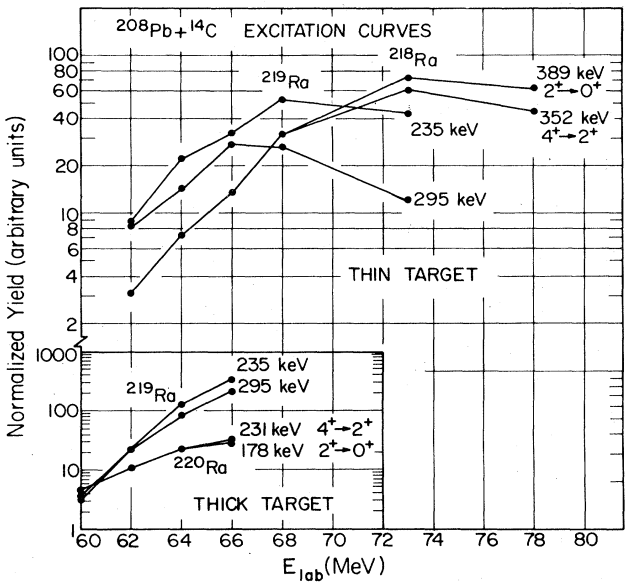

FIG. 1. Excitation functions for selected γ rays from the $^{14}C+^{208}Pb$ reaction.

^{219}Ra. Measurements of excitation functions with the thick self-supporting ^{208}Pb target did, however, clearly show the production of ^{220}Ra (see the inset of Fig. 1).

For the γ-γ coincidence measurements the thick target was used; this enabled us to observe reactions at energies ranging from the beam energy of 68 MeV down to the Coulomb barrier ($\approx$60 MeV). This range of energies allowed the population of high-spin as well as a moderate population of lower-spin states in ^{220}Ra. One HPGe detector of 20% efficiency and two Ge(Li) detectors of 22% and 19% efficiency were employed; the resolutions were 2.0—2.1 keV FWHM at 1.33 MeV. Coincidences between each pair of detectors were recorded on event tapes for off-line analysis; a total of 1.7×10^8 events was collected.

The γ-ray angular distribution measurements were performed with the thick target at two different beam energies. The first measurement was made at 63 MeV with a Compton-suppressed spectrometer consisting of a Ge detector inside a 25.4 cm$\times$20.3 cm NaI(Tl) crystal. Our first results[20] were based on these data; corresponding spectra are shown in Fig. 2. Since that time we have remeasured the angular distributions at a beam energy of 67 MeV using both the Compton-suppressed system and a low energy photon spectrometer (LEPS). Data were taken at six angles between 0° and 90°. Typical beam currents were 4 particle nA, and we acquired data for approximately 8 h at each angle. A spectrum from the LEPS is given in Fig. 3. Because of its superior resolution (0.7 keV FWHM at 122 keV), we were able to resolve several γ rays that had not been resolved in the previous measurement; thus several intensities have been revised from those reported in our earlier work. For γ rays with higher energy and thus low efficiency in the LEPS, spectra from the Compton-suppressed detector were employed as well.

III. EXPERIMENTAL RESULTS

Prior to recent experiments,[18—20] the only known levels of ^{220}Ra were from alpha-decay studies by Ruiz.[21] Three excited states had been identified at excitation energies of 177, 410, and 475 keV with spin and parity assignments of 2^+, 1^-, and 4^+, respectively. The expected production of ^{220}Ra near 60 MeV in the $^{14}C+^{208}Pb$ reaction was confirmed by observation of a 178.1 keV γ ray, corresponding to the $2^+\rightarrow0^+$ transition. Although there is also a 178 keV γ ray in ^{219}Fr,[22] which corresponds to p2n evaporation, we did not observe the stronger 192 keV γ ray which should also be present in the deexcitation of ^{219}Fr. Further confirmation of our identification of ^{220}Ra comes from the reaction ^{208}Pb(^{18}O,α2n) studied by Burrows *et al.*[18]

Coincidence spectra were generated for all detected γ rays; the 178 keV ground-state transition gate is shown in Fig. 4. The angular distribution of each γ ray was fitted to

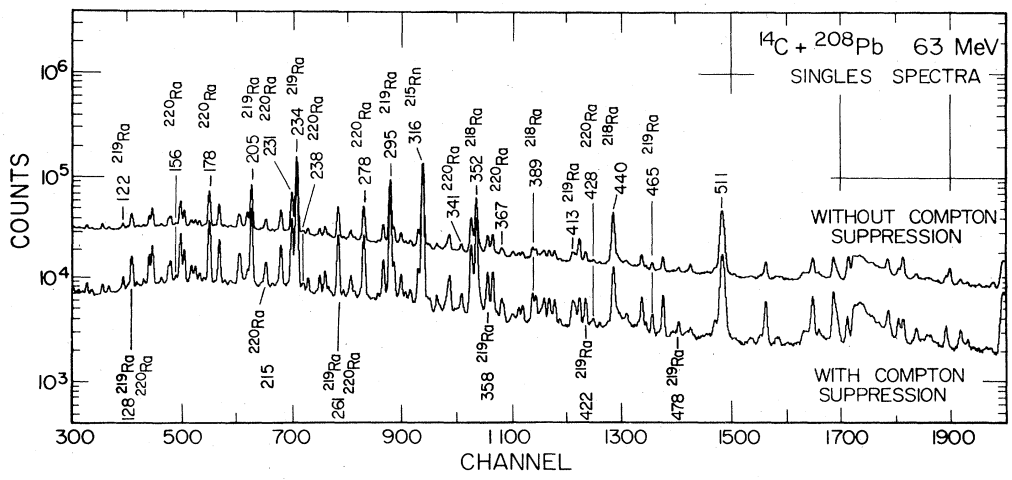

FIG. 2. Singles γ-ray spectra for $^{14}C+^{208}Pb$ at 63 MeV taken with the Compton-suppressed spectrometer. The background is suppressed by approximately a factor of 4.5 at $E_\gamma=100$ keV.

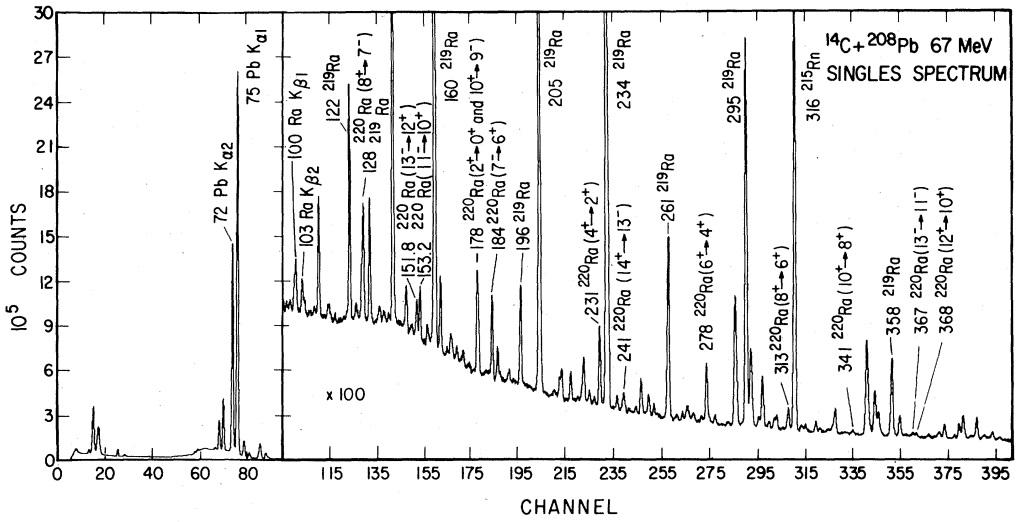

FIG. 3. Singles γ-ray spectrum for $^{14}C+^{208}Pb$ at 67 MeV with the LEPS detector.

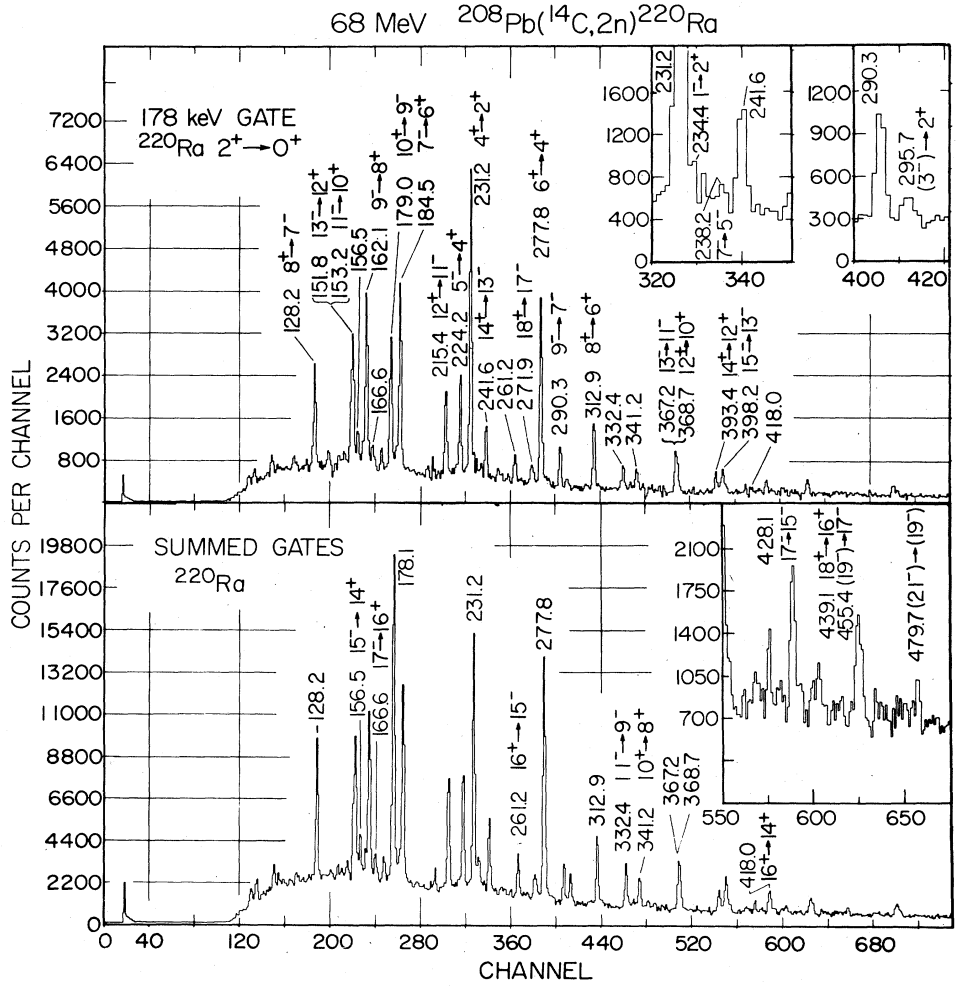

FIG. 4. Coincidence gates for ^{220}Ra. The upper half of the figure shows the spectrum of γ rays in coincidence with the 178 keV $2^+\rightarrow0^+$ transition; note the two insets for details of the $1^-\rightarrow2^+$ and $(3^-)\rightarrow2^+$ γ rays. The lower half represents the sum of the 153, 162, 178, 185, 231, and 367 keV gates and shows several γ rays not observable in any individual gate.

$$W(\theta)=A_0[1+A_2P_2(\theta)+A_4P_4(\theta)] . \quad (1)$$

With information from the coincidence spectra and from the angular distributions, the level scheme shown in Fig. 5 was constructed. Spin assignments were made by assuming that the transitions were stretched, a common assumption in (HI,xn) reactions supported by the large angular momentum involved. Under these assumptions dipole transitions have negative A_2 values and quadrupole transitions positive A_2 values. The experimental values of A_2 and A_4 are listed in Table I for each γ ray in ^{220}Ra, along with the relative intensity and location in the level scheme.

For states with $J>7$, an independent confirmation of the multipolarities was available since each state deexcites by both a quadrupole and a dipole transition. Thus the energy of a quadrupole transition must be the sum of the energies of a pair of dipole transitions; further, the $L=2$ transition cannot be in coincidence with either of the $L=1$ transitions. This information was particularly valuable because many of the γ rays were obscured by strong lines from ^{219}Ra, and thus good angular distributions were unavailable. Because the internal conversion coefficients for electric and magnetic transitions differ so much in this mass region, we are able to differentiate between electric and magnetic transitions on the basis of intensity arguments. From the assignment of the 178 keV transition as electric quadrupole,[21] it follows that all other transitions are also electric.

As a specific example we consider the feeding and deexcitation of the 6^+ state at 687 keV. The 277.8 keV transition deexciting this level has been established as $E2$ by considering the intensity balance for the 4^+ state. Feeding the 6^+ state are γ rays of 184.5 ($L=1$) and 312.9 ($L=2$) keV with γ-ray intensities of 55 ± 1 and 50 ± 2, respectively, relative to the value of $I_\gamma=100$ assigned to the 231.2 keV γ ray. If the 312.9 keV transition is magnetic, its total conversion coefficient is ≈2.25, and its to-

TABLE I. Properties of γ rays observed in ^{220}Ra.

E_γ (keV)[a]	A_2	A_4	I_γ[b]	I_{tr}[c]	$J_f\rightarrow J_i$
128.2	−0.23(3)		29(1)	27(1)	$8^+\rightarrow7^-$
151.8	−0.16(2)		22(1)	19(1)	$13^-\rightarrow12^+$
153.2	−0.22(2)		30(1)	25(1)	$11^-\rightarrow10^+$
156.5	−0.47(5)		10(1)	8(1)	$15^-\rightarrow14^+$
162.1	−0.22(1)		43(1)	35(1)	$9^-\rightarrow8^+$
166.6[e]			5(1)	4(1)	$17^-\rightarrow16^+$
178.1[d]			73(4)	105(5)	$2^+\rightarrow0^+$
179.0[d]			34(4)	26(4)	$10^+\rightarrow9^-$
184.5	−0.21(1)		55(1)	42(1)	$7^-\rightarrow6^+$
215.4	−0.24(4)		23(1)	17(1)	$12^+\rightarrow11^-$
224.2	0.25(20)		15(2)	11(2)	$5^-\rightarrow4^+$
231.2	0.29(1)	−0.07(2)	100	100	$4^+\rightarrow2^+$
234.4[e]			1.0(3)	0.7(2)	$1^-\rightarrow2^+$
238.2[e]			3(1)	3(1)	$7^-\rightarrow5^-$
241.6	−0.11(3)		23(1)	17(1)	$14^+\rightarrow13^-$
261.2[e]			5(1)	4(1)	$16^+\rightarrow15^-$
271.9	−0.49(49)		16(3)	11(2)	$18^+\rightarrow17^-$
277.8[e]			89(6)	75(6)	$6^+\rightarrow4^+$
290.3[e]			17(3)	14(3)	$9^-\rightarrow7^-$
295.7[e]			2(1)	2(1)	$(3^-)\rightarrow2^+$
312.9	−0.06(4)	0.02(5)	50(2)	40(2)	$8^+\rightarrow6^+$
332.4	0.42(2)	−0.30(25)	25(2)	20(2)	$11^-\rightarrow9^-$
341.2	0.39(10)	0.10(13)	12(1)	9(1)	$10^+\rightarrow8^+$
367.2	0.29(9)	−0.30(12)	15(1)	11(1)	$13^-\rightarrow11^-$
368.7	0.20(12)	0.19(18)	11(1)	8(1)	$12^+\rightarrow10^+$
393.4[e]			12(2)	9(2)	$14^+\rightarrow12^+$
398.2	0.36(3)	−0.29(4)	18(1)	13(1)	$15^-\rightarrow13^-$
418.0[f]			4(1)	3(1)	$16^+\rightarrow14^+$
428.1[e]			8(2)	6(2)	$17^-\rightarrow15^-$
439.1			<1	<1	$18^+\rightarrow16^+$
455.4[e]			13(4)	9(3)	$(19^-)\rightarrow17^-$
479.7[e]					$(21^-)\rightarrow(19^-)$

[a]Energies are accurate to ±0.2 keV.
[b]Bare γ-ray intensity relative to 231.2 keV γ ray.
[c]Intensity (including internal conversion) relative to 231.2 keV transition.
[d]Doublet in ^{220}Ra.
[e]Doublet in ^{219}Ra.
[f]Doublet in ^{218}Ra.

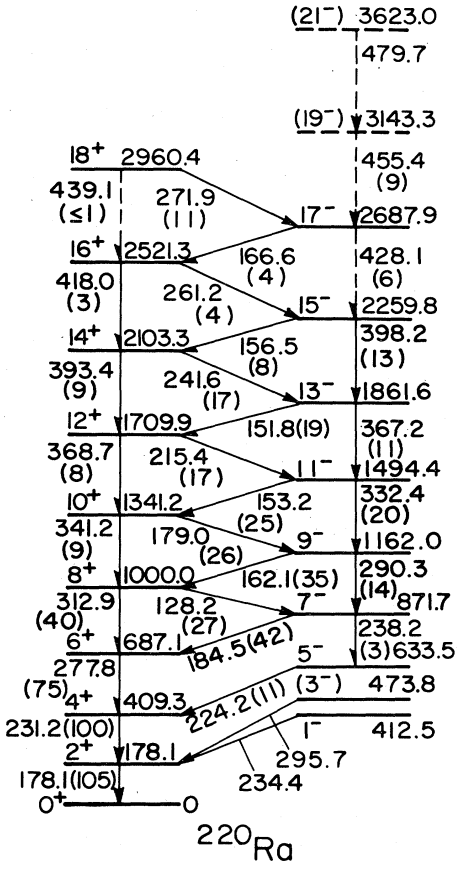

FIG. 5. The level scheme of ^{220}Ra. Numbers in parentheses represent relative intensities, corrected for internal conversion.

tal intensity (relative to a value $I_{tr}=100$ for the $4^+\rightarrow 2^+$ transition) is 111 ± 5. Since this is greater than the value $I_{tr}=75\pm 6$ for the 277.8 keV transition, the $M2$ assumption must be wrong; otherwise the intensity populating the 6^+ state would exceed the intensity depopulating it. If the dipole transition is magnetic, its conversion coefficient is ≈ 2.9, and $I_{tr}=147\pm 3$; again the feeding would be too large. Thus both transitions observed feeding the 6^+ state must be electric, and the conversion coefficients are 0.12 and 0.17 for the dipole and quadrupole transitions, respectively. Intensities are $I_{tr}=42\pm 1$ for the 184.5 keV transition and $I_{tr}=40\pm 2$ for the 312.9 keV transition. The sum is 82 ± 4 and agrees well with the deexciting intensity of 75 ± 6.

Also shown in Fig. 4 is the sum of six of the coincidence gates. This summing allowed the assignment of several additional γ rays to ^{220}Ra, although their exact placement in the level scheme was not possible without further coincidence information. However, based on the systematics of the negative-parity states, we are able to make tentative assignments and show them by dashed lines in Fig. 5.

Finally, some comments on the low-spin states are in order. The largest peak in the 178 keV coincidence spectrum corresponds to the 231.2 keV quadrupole transition, and we accordingly assign this as $4^+\rightarrow 2^+$. This placement of the 4^+ at 409.3 keV contradicts Ruiz's assignment. However, a weakly populated level at 473.8 keV is probably the state assigned 4^+ in the alpha-decay work; based on a similarly located state in ^{218}Ra,[3] we tentatively classify this level as $J^\pi=3^-$. There is also some evidence (see the inset of Fig. 4) for a weak γ ray of 234.4 keV in coincidence with the $2^+\rightarrow 0^+$ transition; we believe that this is the $1^-\rightarrow 2^+$ transition observed by Ruiz and therefore place a 1^- state at 412.5 keV.

Our results are in good agreement with those obtained from other studies of ^{220}Ra.[18,19] We observed all states which were identified in those studies. In addition, we include the two low-lying levels at 412 and 474 keV and the two tentatively identified states at 3143 and 3623 keV.

IV. DISCUSSION

The level schemes of ^{214}Ra (Ref. 23), ^{216}Ra (Refs. 24 and 25), ^{218}Ra (Refs. 2–4), ^{220}Ra, and ^{222}Ra (Ref. 22) are shown in Fig. 6; the changes are dramatic as N increases from 126 to 134. The excitation energy of the 2_1^+ state decreases by roughly a factor of 2 each time two additional neutrons are added, indicating the well-known importance of the neutron-proton interaction for the onset of collectivity in transition nuclei. Despite this decrease in energy, deformation does not yet play a major role; in ^{220}Ra the value of $E(4_1^+)/E(2_1^+)$ is 2.3, still close to the value of 2.0 characteristic of vibrational nuclei. However, a more important feature of these level schemes is the location of the negative-parity states. In ^{214}Ra and ^{216}Ra the lowest observed negative-parity states have $J^\pi=11^-$ and have been interpreted as two-quasiparticle proton states.[23–25] On the other hand, the three heavier isotopes show negative-parity states which are substantially lower in both spin and excitation energy; 1^- states below 1 MeV have been identified (tentatively in ^{218}Ra) in each of these nuclei. The change in structure is even more apparent from the sequences of states of alternating parity in ^{218}Ra and ^{220}Ra.

In Fig. 7 we plot J_x, the component of angular momentum along the rotation axis,[12] as a function of the rotational frequency for ^{218}Ra and ^{220}Ra. Again there is clear evidence for a change in the structure as the neutron number increases. For the negative-parity states in ^{218}Ra, there is a sharp increase in J_x above $J^\pi=11^-$. This appears to be the result of a band crossing since the curve has a smooth continuation (indicated by the dashed line in Fig. 7) if we include some tentatively assigned nonyrast levels.[4] The fact that this sharp discontinuity in the curve occurs at the 11^- state leads us to suggest that the two-quasiparticle state present in both ^{214}Ra and ^{216}Ra also plays a role in the structure of ^{218}Ra. In ^{220}Ra J_x increases smoothly for both positive-parity and negative-parity states, and there is no sign of any effect of a two-quasiparticle state.

Still further evidence for the transition taking place in this region is shown in Fig. 8, where we plot $B(E1)/B(E2)$ for ^{218}Ra, ^{220}Ra, and ^{226}Ra (Ref. 26) as a function of J. Several effects appear to be present. For states with $J\leq 11$, the ratios appear to be roughly con-

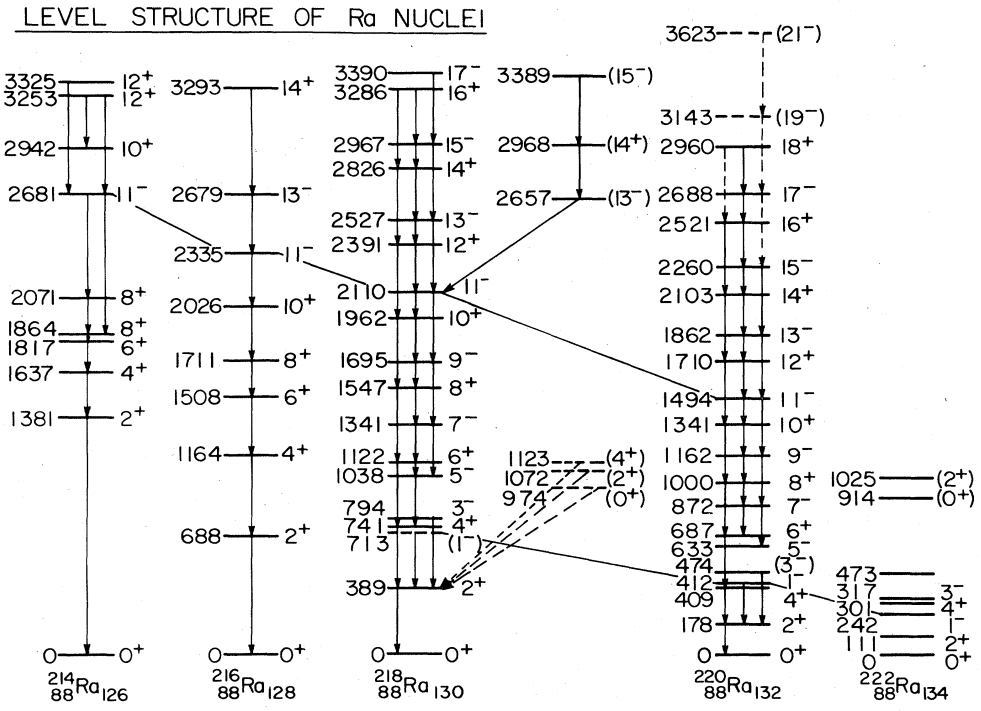

FIG. 6. Systematics of the energy levels for light even-even Ra isotopes. Data are from Refs. 3 and 4, 22—25, and the present work. Note particularly the low-lying 1^- and high-lying 11^- states as discussed in the text.

stant for ^{218}Ra and ^{220}Ra and increasing with J for ^{226}Ra. In both ^{218}Ra and ^{220}Ra, the values of this ratio are strongly enhanced, offering evidence that the $E1$ strength is of collective origin. However, the average value of $B(E1)/B(E2)$ decreases by a factor of ≈ 2.5 for ^{220}Ra, relative to ^{218}Ra, and by roughly another order of magnitude for ^{226}Ra. Measurements[5] of lifetimes in ^{218}Ra give values of $B(E2)\approx 70$ W.u.; to attribute the decrease in the ratio for the states in ^{220}Ra solely to an increase in $B(E2)$ then requires a rather large value of $B(E2)$ (≈ 175 W.u.). On this basis we suggest that these $E1$ matrix elements decrease slightly as A increases.

For the higher spin states in ^{218}Ra, the behavior of $B(E1)/B(E2)$ changes; the ratio appears to decrease. This decrease may reflect the change in structure due to the band crossing at $J=11$ discussed earlier. Since the

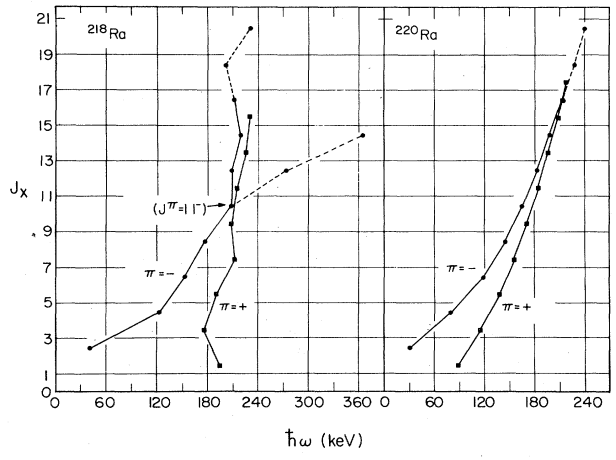

FIG. 7. Component of J along the x axis versus angular frequency for ^{218}Ra and ^{220}Ra.

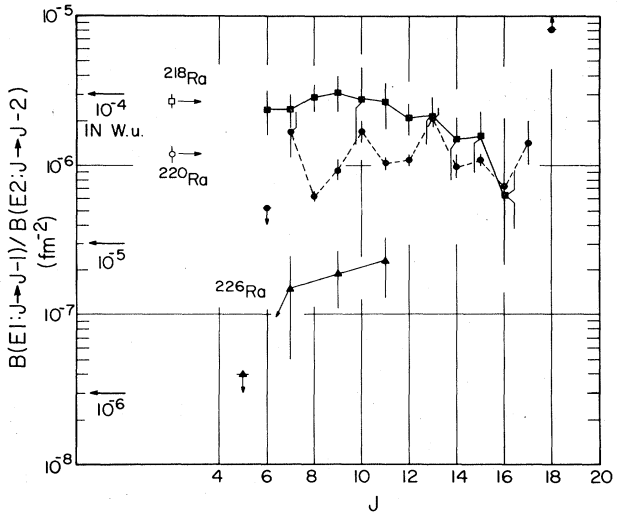

FIG. 8. $B(E1)/B(E2)$ for states in ^{218}Ra, ^{220}Ra, and ^{226}Ra. Average values for states with $J\leq 11$ in ^{218}Ra and ^{220}Ra are denoted by open symbols. Units on the ordinate axis are fm^{-2}, and equivalent values are shown when the $B(E\lambda)$ are in Weisskopf units. Data are from Refs. 3 and 26 and the present work.

states based on a two-quasiparticle configuration would be less collective than the lower spin states, this decrease in $B(E1)/B(E2)$ offers further evidence that the dipole transitions are collective in nature.

It was recognized very early that low-lying negative-parity states could be described by an octupole degree of freedom,[27] and many studies have explored this possibility (see Ref. 11 for an extensive list). Early calculations, e.g., Ref. 28, found no evidence for a stable octupole deformation, and thus many calculations based on a vibrational mode were performed. However, the lack of experimental evidence for 0^+ states corresponding to the two-phonon vibration[29,30] has called this interpretation into question near $A=220$. Moreover, Möller and Nix[31] recently found, for the first time, theoretical evidence for a stable octupole deformation near ^{222}Ra, and subsequent calculations[11,13] have shown minima in potential energies for $\beta_3 \neq 0$ in the Ra isotopes with $A \approx 220$–228. Some of the consequences for high-spin states of octupole deformation have been discussed by Nazarewicz *et al.*[12,14]

Another theoretical approach to this mass region, the vibron model,[8] has been formulated in terms of alpha clustering and the group structure U(6)⊗U(4). Here the emphasis is on a dipole rather than an octupole mode. In addition to the s,d bosons of the standard interacting boson model,[32] this model employs s^* and p^* bosons to describe the dipole degree of freedom. States from a configuration with no alpha particle (only s,d bosons) are mixed with states from a configuration with one alpha particle (two s^*,p^* bosons) in order to obtain eigenvectors which describe the interplay of the quadrupole and dipole degrees of freedom. Observables can then be calculated and compared to experimental data; several calculations[9,10] have been performed for Ra and Th isotopes within the framework of this model.

In Fig. 9 we present the results of vibron model calculations for the nuclei ^{220}Ra, ^{222}Ra, ^{224}Ra, and ^{226}Ra. The Hamiltonian used is that described in Ref. 9, and our parameters are listed in Table II. Unlike the previous calculations, which have varied several parameters in moving from isotope to isotope, we vary *only* the parameter ϵ_p (the energy of a single p^* boson) to obtain these fits. The total number of bosons for each nucleus is the number of pairs of nucleons outside the $Z=82$ and $N=126$ shell closures; this method of counting means that the higher-spin states are outside the scope of this model. Furthermore, the lack of knowledge about levels in ^{222}Ra and ^{224}Ra limits a stringent test of the model for these nuclei. Howev-

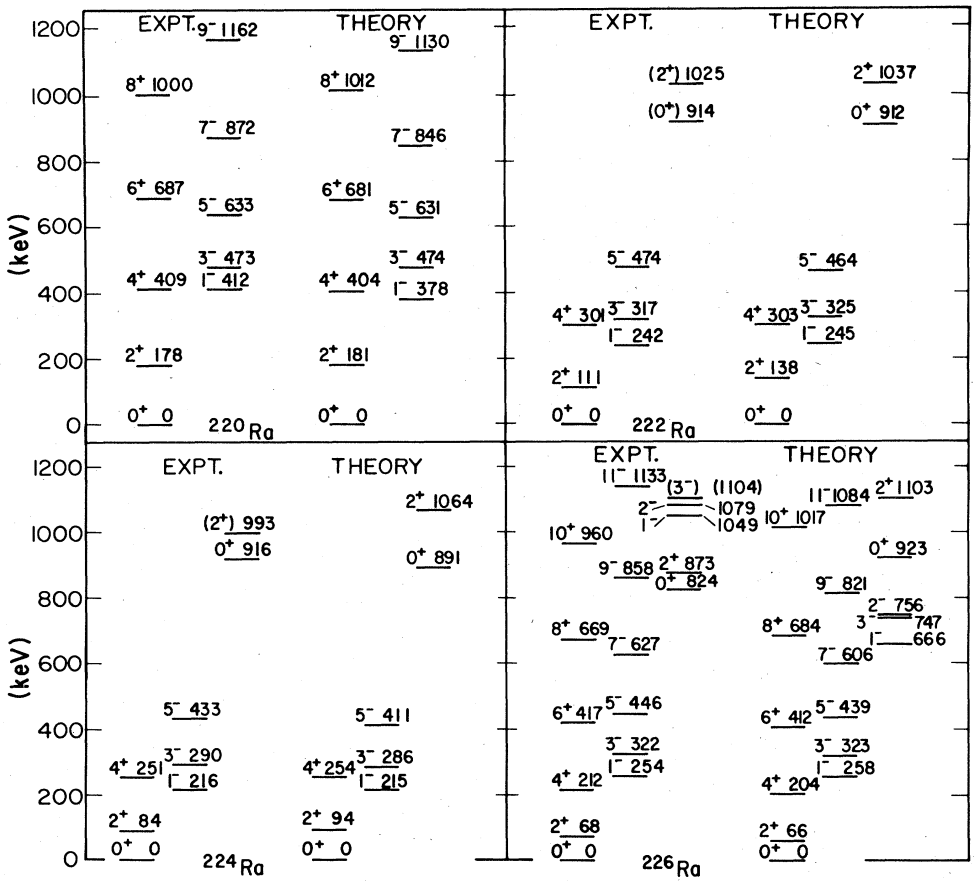

FIG. 9. Comparison of energy levels predicted by the vibron model to experimental levels for ^{220}Ra, ^{222}Ra, ^{224}Ra, and ^{226}Ra. Parameters used in the fits are listed in Table II. Note that only one parameter was varied for the different isotopes, as discussed in the text. All experimentally known levels with spins allowed by the constraints from boson number are included.

TABLE II. Parameters used in the vibron model fits shown in Fig. 9.

ϵ_d	0.180	MeV
κ_d	−0.085	MeV
$\kappa'(^{A}\mathrm{Ra})$	0.006	MeV
$\kappa'(^{A-4}\mathrm{Rn}+\alpha)$	0.0036	MeV
ϵ_p ^{220}Ra	0.02	MeV
^{222}Ra	−0.12	MeV
^{224}Ra	−0.14	MeV
^{226}Ra	0.10	MeV
α_p	1.000	MeV
κ	−0.030	MeV
Δ_α	−0.25	MeV
γ	−0.080	MeV
χ	−2.25	

er, the calculations, in general, reproduce the excitation energies quite well, including those of the low-lying negative-parity states, and seem to provide a reasonable description of these nuclei (although the quality is not as good as the fits of Daley *et al.*[9,10]). It is interesting to note that we cannot reproduce the excitation energies of ^{218}Ra with the same parameters; this suggests again a transition in structure taking place in this region, although it may simply reflect the effects of the small number of bosons in ^{218}Ra.

In addition to reproducing the energy levels, the cluster model offers a simple understanding of the large reduced alpha widths observed in this mass region.[33] One can also examine the role of clustering in terms of a molecular sum rule.[17] In ^{220}Ra the estimated $B(E1)$ exhausts $\approx 2\%$ of this sum rule.

The same features of the Ra isotopes can also be understood in terms of the octupole model. Nazarewicz *et al.*[13] have examined the question of octupole deformation in several mass regions; they conclude that octupole deformation may be particularly important for nuclei near ^{224}Th and that the energy of the lowest negative-parity state is correlated with the degree of deformation. They also suggest that at high spins nuclei may become more stable with respect to octupole deformation, and therefore a nucleus such as ^{220}Ra which appears to be spherical in its ground state[13] may move toward both quadrupole and octupole deformation with increasing rotational frequency. Another prediction of the octupole theory[12] is that the data should show an upbend but no backbend. Figure 7 clearly shows such behavior in ^{220}Ra.

Since many of the predictions of the two models are similar, it is important to understand the relation between them. In the octupole model the introduction of the octupole degree of freedom leads to a dipole moment. In the vibron model it is the dipole degree of freedom which is explicitly introduced via the cluster configuration, and this in turn leads[17] to a quadrupole moment, octupole moment, etc. The available experimental data do not permit at present a clear distinction between the two interpretations. Engel and Iachello[34] have recently proposed a scheme based on the group U(16) to describe even-even nuclei with octupole shapes in the hope that this may allow a more quantitative comparison of the two ideas. In this model any number of f bosons are allowed, subject to the constraint on the total number of bosons. One of their findings is that smooth rotational bands cannot be generated by inclusion of f bosons alone but require p bosons as well. Thus this approach suggests from a group theoretical standpoint the need for both dipole and octupole degrees of freedom. They suggest that data on bands built on excited states may prove useful in resolving this question; however, such measurements are difficult near $A=220$ because of the strong selectivity of (HI,xn) reactions for yrast levels.

Catara *et al.*[35] have recently considered surface clustering in heavy deformed nuclei in terms of particles in Nilsson orbitals and of pairing interactions. They conclude that pairing enhances the clustering, although calculated spectroscopic factors are still too small. Nonetheless, the emphasis on single-particle levels suggests a connection with the octupole model, where the theoretical understanding of octupole deformation relies upon the available single-particle levels and their interaction via a Y_{30} term.[13] If we consider odd-mass nuclei, interpretations have focused upon the octupole description;[36,37] the model provides a simple understanding of the parity doublets observed in several of the actinide nuclei and has also been applied to properties such as ground state spins and parities, magnetic moments, and decoupling parameters. The vibron model has not been extended to odd-mass nuclei, and thus such comparisons cannot be made with it.

In conclusion, more data seem necessary to firmly establish one or the other of the models near $A=220$. Systematics over a wide range of nuclei should provide more stringent tests than currently available. Greater theoretical understanding of the relationship between the vibron model and the octupole model would prove most useful in devising experimental tests.

ACKNOWLEDGMENTS

We wish to thank P. Thieberger and R. Lindgren of the Brookhaven National Laboratory for developing and providing the ^{14}C beam and the staff of the tandem lab at the University of Munich for providing the ^{14}C pellets. This work was supported in part by the U.S. D.O.E. under Contract Nos. DE-AC02-76ER03074 and DE-AC02-76CH00016 and by the NSF.

[1]F. S. Stephens, Jr., Frank Asaro, and I. Perlman, Phys. Rev. **100**, 1543 (1955).

[2]J. Fernandez-Niello, H. Puchta, F. Riess, and W. Trautmann, Nucl. Phys. **A391**, 221 (1982).

[3]M. Gai, J. F. Ennis, M. Ruscev, E. C. Schloemer, B. Shivakumar, S. M. Sterbenz, N. Tsoupas, and D. A. Bromley, Phys. Rev. Lett. **51**, 646 (1983).

[4]Y. Itoh, Y. Gono, M. Sasagase, T. Kubo, M. Sugawara, S.

Hayashibe, K. Hiruta, T. Kono, and T. Nomura, RIKEN Internal Report, 1982 (unpublished), Vol. 16, p. 48; Y. Gono, private communication.

[5]J. F. Ennis, M. Gai, D. A. Bromley, F. Azgui, H. Emling, E. Grosse, G. Seiler-Clark, H. J. Wollersheim, C. Mittag, and F. Riess, Bull. Am. Phys. Soc. **29**, 1050 (1984).

[6]W. Bonin, M. Dahlinger, S. Glienke, E. Kankeleit, M. Krämer, D. Habs, B. Schwartz, and H. Backe, Z. Phys. A **310**, 249 (1983).

[7]D. Ward, G. D. Dracoulis, J. R. Leigh, R. J. Charity, D. J. Hinde, and J. O. Newton, Nucl. Phys. **A406**, 591 (1983).

[8]F. Iachello and A. D. Jackson, Phys. Lett. **108B**, 151 (1982).

[9]H. Daley and F. Iachello, Phys. Lett. **131B**, 281 (1983).

[10]Henry J. Daley and Moshe Gai, Phys. Lett. **149B**, 13 (1984).

[11]G. A. Leander, R. K. Sheline, P. Möller, P. Olanders, I. Ragnarsson, and A. J. Sierk, Nucl. Phys. **A388**, 452 (1982).

[12]W. Nazarewicz, P. Olanders, I. Ragnarsson, J. Dudek, and G. A. Leander, Phys. Rev. Lett. **52**, 1272 (1984).

[13]W. Nazarewicz, P. Olanders, I. Ragnarsson, J. Dudek, G. A. Leander, P. Möller, and E. Ruchowska, Nucl. Phys. **A429**, 269 (1984).

[14]W. Nazarewicz and P. Olanders, Phys. Rev. C **32**, 602 (1985).

[15]V. M. Strutinski, At. Energ. **1**, 150 (1956) [Sov. J. At. Energy **4**, 523 (1957)].

[16]A. Bohr and B. R. Mottelson, Nucl. Phys. **4**, 529 (1957); **9**, 687 (1958).

[17]Y. Alhassid, M. Gai, and G. F. Bertsch, Phys. Rev. Lett. **49**, 1482 (1982).

[18]J. D. Burrows, P. A. Butler, K. A. Connell, A. N. James, G. D. Jones, A. M. Y. El-Lawindy, T. P. Morrison, J. Simpson, and R. Wadsworth, J. Phys. G **10**, 1449 (1984).

[19]A. Celler, Ch. Briançon, J. S. Dionisio, A. Lefebvre, Ch. Vieu, J. Zylicz, R. Kulessa, C. Mittag, J. Fernandez-Niello, Ch. Lauterbach, H. Puchta, and F. Riess, Nucl. Phys. **A432**, 421 (1985).

[20]P. D. Cottle, J. F. Shriner, Jr., F. Dellagiacoma, J. F. Ennis, M. Gai, D. A. Bromley, J. W. Olness, E. K. Warburton, L. Hildingsson, M. A. Quader, and D. B. Fossan, Phys. Rev. C **30**, 1768 (1984).

[21]Carl Phillip Ruiz, Ph.D. thesis, University of California, Berkeley, 1961 [University of California, Berkeley Report No. UCRL 9511, 1961 (unpublished)].

[22]*Table of Isotopes,* 7th ed., edited by C. M. Lederer and V. S. Shirley (Wiley, New York, 1978).

[23]D. Horn, O. Häusser, B. Haas, T. K. Alexander, T. Faestermann, H. R. Andrews, and D. Ward, Nucl. Phys. **A317**, 520 (1979).

[24]A. Chevallier, J. Chevallier, B. Haas, S. Khazrouni, and N. Schulz, Z. Phys. A **308**, 277 (1982).

[25]Y. Itoh, Y. Gono, T. Kubo, M. Sugawara, and T. Nomura, Nucl. Phys. **A410**, 156 (1983).

[26]C. Mittag, R. Zimmerman, and J. deBoer, University of Munich Annual Report, 1980 (unpublished); R. Zimmerman, Ph.D. thesis, University of Munich, 1980.

[27]K. Alder, A. Bohr, T. Huss, B. Mottelson, and A. Winther, Rev. Mod. Phys. **28**, 432 (1956).

[28]P. Vogel, Nucl. Phys. **A112**, 583 (1968).

[29]W. Kurcewicz, E. Ruchowska, J. Zylicz, N. Kaffrell, and N. Trautmann, Nucl. Phys. **A304**, 77 (1978).

[30]W. Kurcewicz, E. Ruchowska, N. Kaffrell, T. Björnstad, and G. Nyman, Nucl. Phys. **A356**, 15 (1981).

[31]Peter Möller and J. Rayford Nix, Nucl. Phys. **A361**, 117 (1981).

[32]A. Arima and F. Iachello, Ann. Phys. (N.Y.) **99**, 253 (1976); **111**, 201 (1978); **123**, 468 (1979).

[33]E. Roeckl, Nucl. Phys. **A400**, 131c (1983).

[34]J. Engel and F. Iachello, Phys. Rev. Lett. **54**, 1126 (1985).

[35]F. Catara, A. Insolia, E. Maglione, and A. Vitturi, Phys. Lett. **149B**, 41 (1984).

[36]G. A. Leander and R. K. Sheline, Nucl. Phys. **A413**, 375 (1984).

[37]G. A. Leander, P. B. Semmes, and F. Dönau, in *Interacting Boson-Boson and Boson-Fermion Systems,* edited by O. Scholten (World Scientific, Singapore, 1984), p. 167.